Prediction of plastic yield surface for porous materials by a machine learning approach

Wanqing Shen, Y.J. Cao, Jian-Fu Shao, Z.B. Liu

Version of Record: https://www.sciencedirect.com/science/article/pii/S2352492820324880
Manuscript_b7218c5a0872c4d5dc6e73baa6d20950

Prediction of plastic yield surface for porous materials by a machine learning approach

W.Q. Shen[a,b,*], Y.J. Cao[c], J.F. Shao[a,b,*], Z.B. Liu[a]

[a] *Key Laboratory of Ministry of Education on Safe Mining of Deep Metal Mines, College of Resources and Civil Engineering, Northeastern University, Shenyang, 110819, China*
[b] *Univ. Lille, CNRS, Centrale Lille, UMR 9013 - LaMcube - Laboratoire de Mécanique, Multiphysique, Multi-échelle, F-59000 Lille, France*
[c] *Key Laboratory of Ministry of Education for Geomechanics and Embankment Engineering, HOHAI University, Nanjing 210098, China*

Abstract

The present paper focuses on the prediction of effective plastic yield surface of porous materials having a von Mises type solid matrix. Some typical explicit yield criteria obtained by different analytical homogenization methods are briefly reviewed and evaluated by using numerical results obtained from direct finite element simulations with different values of porosity. Each criterion has its own advantage and weakness. In order to get a better prediction, the Artificial Neuron Network (ANN) algorithm is adopted specially for the prediction of macroscopic yield stress of porous materials, seen as a regression problem with two input parameters and one output value. For the training purpose which is a key step in the ANN approach, new numerical results are presented in the present work with a wide range of porosity and of macroscopic stress triaxiality. Based on these data, the ANN approach is trained and it converges quickly. Then the ANN predictions are compared with numerical test data, a good agreement is found for all loading cases. Comparing with the existing yield criteria, the prediction given by the ANN approach is much more accuracy and easy to apply.

Keywords: Yield surface, Artificial neuron network, Machine learning, Porosity, Porous material, Micro-mechanics

*Corresponding authors: wanqing.shen@polytech-lille.fr jian-fu.shao@polytech-lille.fr,

1. Introduction

In recent decades, the investigation of pore influence on the material strength is one of the most popular research topics. Even with low porosity, the material mechanical behavior can be affected importantly and the resistance will reduce quickly. It is thus crucial to take into account the pore effect on the safety and durability analysis of structure. For this purpose, many researches have developed: analytical approaches, numerical simulations or experimental measurements. In the analytical study, different methods have been proposed by researchers to study the influence of pore on the macroscopic mechanical behavior of porous materials. Among these, the pioneer's work has been realized by [1]. In the framework of limit analysis with a kinematical velocity field, an analytical macroscopic strength criterion has been obtained by considering a hollow sphere or cylinder with a von Mises type incompressible solid matrix. In order to better fit experimental evidences and numerical results, a number of extensions of this criterion have been proposed. For example, by introducing some heuristic modifications of the Gurson's criterion [2, 3], the so-called GTN (Gurson-Tvergaard-Needelman) model has been established and widely used in various applications. Based on the non-linear variational homogenization techniques, [4] proposed an elliptic macroscopic yield criterion. Comparing with the Gurson's criterion, it appears more accuracy for the deviatoric loading and less accuracy for the hydrostatic loading. This feature was improved by [5] and other researchers. By adopting the Eshelby-like velocity fields, an improvement based on micromechanics has been achieved in [6] and the deviatoric prediction is ameliorated. Recently, a stress variational method has been proposed in [7] for the derivation of macroscopic yield criterion for the porous material with a von Mises matrix. It is improved in [8] by construction of a totally statically admissible stress field. There are many other extensions, such as for accounting for the pore shape [9–14], for pressure-sensitive materials [14–22], for two populations of pore at different scales [23–28], and son on, just to mention a few.

In the derivation of effective yield criteria for porous materials, each approach has its own advantage and disadvantage. To construct a suitable yield criterion which fully takes

into account the pore effect is really a hard task. Recently, the machine learning based approaches have been developed very quickly. For example, one can mention the artificial neuron network (ANN) inspired from the biological structure of neurons [29]. Based on the training data, the ANN approach can "learn" itself the inherent rules of things which are cashed behind the training data. This method has been applied to many areas. In [30], the behaviour of concrete in the state of plane stress under monotonic biaxial loading and uniaxial compressive cyclic loading were studied by the neuron network; an implicit viscoplastic constitutive model based on neuron network was proposed in [31] for the inelastic behavior of material; the non-linear mechanical behaviors of heterogeneous materials were investigated in [32, 33] by the deep material networks; the structure analysis was presented in [34] by the deep learning method, just mention a few. Differently from the traditional methods for the derivation of yield criteria, the artificial neuron network method will be used in this work to study the macroscopic mechanical behavior of porous materials. The influence of porosity on the effective behavior will be fully investigated, and in particular the relations between the deviatoric and hydrostatic stresses.

There are three principal parts in this paper which is organised as follows: a brief recall of some typical macroscopic yield criteria for porous materials with a von Mises solid matrix obtained by different methods is first presented in section 2; section 3 introduces the numerical model for the porous material used for direct finite element simulations, which are used to evaluate the accuracy of the selected analytical yield criteria and also for the preparation of training data which will be used in the artificial neuron network approach; the ANN approach is used in section 4 for the studied porous material and its predictions are compared with the finite element reference results and the analytical solutions; a concluding remark is given in section 5.

2. Brief recall of some typical theoretical yield criteria of porous medium

In order to study analytically the influence of porosity on the macroscopic plastic yield behavior of porous materials, a hollow sphere with inner radius a and outer one b is often chosen as a representative volume element. At the microscopic scale, the volume of the pore

is denoted as V_p, the one of the matrix is V_m. The corresponding porosity of the studied porous medium can be calculated as $f = \frac{V_p}{V_p+V_m} = \frac{a^3}{b^3}$. The behavior of matrix is perfectly elasto-plastic and obeys to a von Mises local yield criterion:

$$\phi(\boldsymbol{\sigma}) = \sigma_{eq} - \sigma_0 \leq 0 \tag{1}$$

where $\boldsymbol{\sigma}$ is the local stress in the matrix at the microscopic scale. $\boldsymbol{\sigma}'$ is the deviatoric part. $\sigma_{eq} = \sqrt{\frac{3}{2}\boldsymbol{\sigma}' : \boldsymbol{\sigma}'}$ denotes the von Mises equivalent stress; σ_0 is the material strength in the case of purely shear loading.

For the studied porous material with a rigid elasto-plastic von Mises type matrix, many analytical macroscopic yield criteria which take into account the effect of porosity have been derived by different methods. Here we firstly do a brief recall of some typical ones.

- Gurson's criterion by limit analysis approach [1]

  For a class of porous materials represented by hollow sphere with a von Mises type incompressible solid matrix, a macroscopic yield criterion was firstly proposed by [1] in the framework of limit analysis with a kinematical velocity field. This criterion considers explicitly the effect of porosity f on the effective behavior.

$$\frac{\Sigma_{eq}^2}{\sigma_0^2} + 2f\cosh\left(\frac{3\Sigma_m}{2\sigma_0}\right) - 1 - f^2 = 0 \tag{2}$$

  in which $\boldsymbol{\Sigma}$ is the stress of porous medium at the macroscopic scale. $\Sigma_{eq} = \sqrt{\frac{3}{2}\boldsymbol{\Sigma}' : \boldsymbol{\Sigma}'}$ is the macroscopic von Mises equivalent stress; Σ_m denotes the macroscopic mean stress with $\Sigma_m = \frac{\Sigma_{11}+\Sigma_{22}+\Sigma_{33}}{3}$ Then many extensions have been done based on this work. For example, comparing with the numerical results obtained from direct simulation, the criterion (2) was improved heuristically by [2, 3] with three parameter q_1, q_2 and q_3.

- Criterion derived in [6] with new velocity fields

  By considering the Eshelby-like velocity fields, a micromechanics-based modification of the Gurson criterion was derived in [6]:

$$\left(1 + \frac{2}{3}f\right)\frac{\Sigma_{eq}^2}{\sigma_0^2} + 2f\cosh\left(\frac{3\Sigma_m}{2\sigma_0}\right) - 1 - f^2 = 0 \tag{3}$$

Comparing with the Gurson's criterion (2), a different deviatoric prediction is given by (3).

- Criterion derived by non-linear variational homogenization techniques [4]

  On other hand, a macroscopic elliptic yield criterion has been derived in [4] by adopting the non-linear variational homogenization techniques:

$$\left(1+\frac{2}{3}f\right)\frac{\Sigma_{eq}^2}{\sigma_0^2}+\frac{9f}{4}\frac{\Sigma_m^2}{\sigma_0^2}-(1-f)^2=0 \tag{4}$$

  This criterion is improved in [5] by retrieving the exact solution in pure hydrostatic loading:

$$\left(1+\frac{2}{3}f\right)\frac{\Sigma_{eq}^2}{\sigma_0^2}+\frac{9}{4}\left(\frac{1-f}{\ln(f)}\right)^2\frac{\Sigma_m^2}{\sigma_0^2}-(1-f)^2=0 \tag{5}$$

- Criterion based on a stress variational method

  In [7], a stress variational method is proposed for deriving the macroscopic criterion of the studied porous materials. This model was improved in [8] with a totally statically admissible stress field:

$$\sqrt{\frac{P_0(f)}{(1-f+P_1)^2}\Sigma_e^2+\frac{9}{4\ln(f)^2}\Sigma_m^2}\;\xi(\zeta)-\sigma_0=0 \tag{6}$$

  where the parameters $P_0(f)$, P_1 and ξ are given in Appendix A.

Different criteria obtained by different method have their own advantages and disadvantages. For example, the exact solution of the pure hydrostatic loading can be retrieved by (2), but overestimated by (4). These criteria will be compared in the following section with finite element solutions.

3. FEM numerical method for the studied porous materials

For the purpose of the evaluations of these criteria and better understand the mechanical behavior of studied porous medium, finite element method (FEM) are often carried out as reference results.

The representative volume element of porous material is here represented by a hollow sphere. Due to its axi-symmetric property, only a quarter of the hollow sphere is considered and it is meshed with 900 quadratic quadrilateral elements of type CAX8 and with 2821 nodes in Abaqus software, as illustrated in Figure 1(a) for the case $f = 0.15$. The solid matrix obeys the von Mises criterion (1). With the assumption of small strains, the displacement velocity field is prescribed on the exterior boundary of the hollow sphere. A user subroutine MPC (Multi-Points Constraints) is used in this study for the loading condition with a constant macroscopic stress triaxiality $T = \Sigma_m/\Sigma_{eq}$, which is realized by calculating the constant stress ratio Σ_ρ/Σ_z as the one done in [17, 35].

In Figure 1(b), the FEM solutions (blue circles) is compared with the lower bounds (red squares) and upper ones (green rhombus) proposed in [36, 37] for porosities $f = 0.01$ and 0.1. The black triangle are exact solutions in the pure hydrostatic loading. The proposed FEM solutions retrieve well the exact results and locate well in the lower and upper bounds. Especially for the case of $f = 0.1$, the upper bound coincides well with the lower bound, which means they approach to the exact solutions. The FEM method has a good precision.

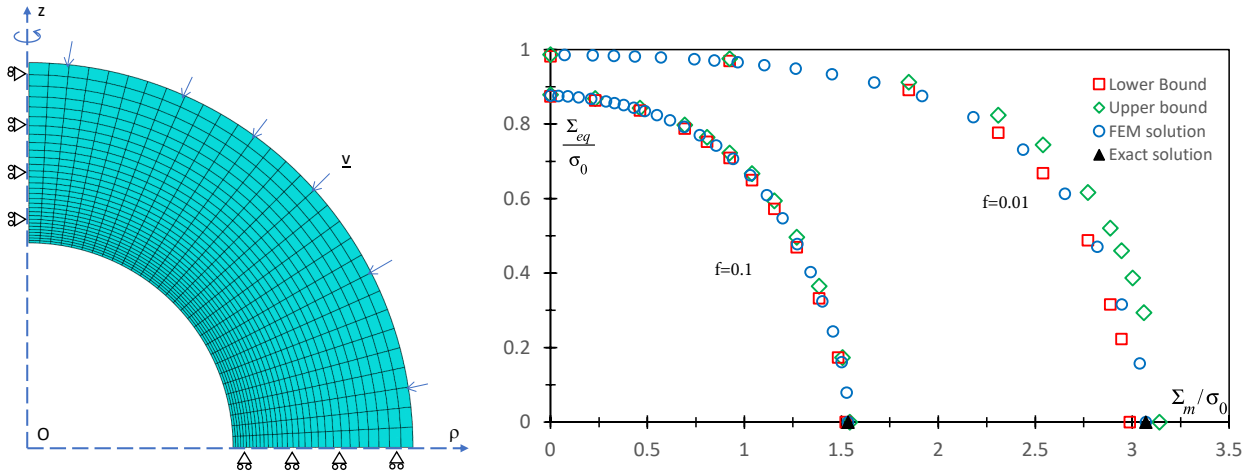

(a) Numerical model with $f = 0.15$

(b) Comparisons for $f = 0.01$ and $f = 0.1$

Figure 1: Validations of the FEM results (blue circles) by the upper (green rhombus) and lower (red squares) bounds proposed by [36, 37], the black triangle is the exact solution in the pure hydrostatic loading.

The macroscopic yield criteria presented in section 2 are evaluated and assessed by the FEM results with different porosities, for example, $f = 0.05,\ 0.1,\ 0.2,\ 0.4$. As illustrated in Figure 2, the black line is the yield surface predicted by the Gurson's criterion (2), the red line is the one given by criterion (3) and orange, green and blue lines are presented by criteria (4), (5), (6), respectively. One can see that different criterion obtained by different approach has its own advantage and disadvantage. For low porosity, criteria (4), (3), (5) and (6) has a good prediction of $\frac{\Sigma_{eq}}{\sigma_0}$ for pure deviatoric loading, the one given by (2) is overestimated. But with the increase of the porosity, this value is underestimated by (4), (3), (5). It seems that the criterion (6) has a good prediction of $\frac{\Sigma_{eq}}{\sigma_0}$ when $\frac{\Sigma_m}{\sigma_0} = 0$ for all porosity f. For intermediate value of stress triaxiality $T = \Sigma_m/\Sigma_{eq}$, the yield surface given by (6) is under the FEM solution when $f = 0.05$, but it is over the FEM solution when $f = 0.2$ and 0.4. In the pure hydrostatic loading, all criteria can retrieve the exact solution except (4).

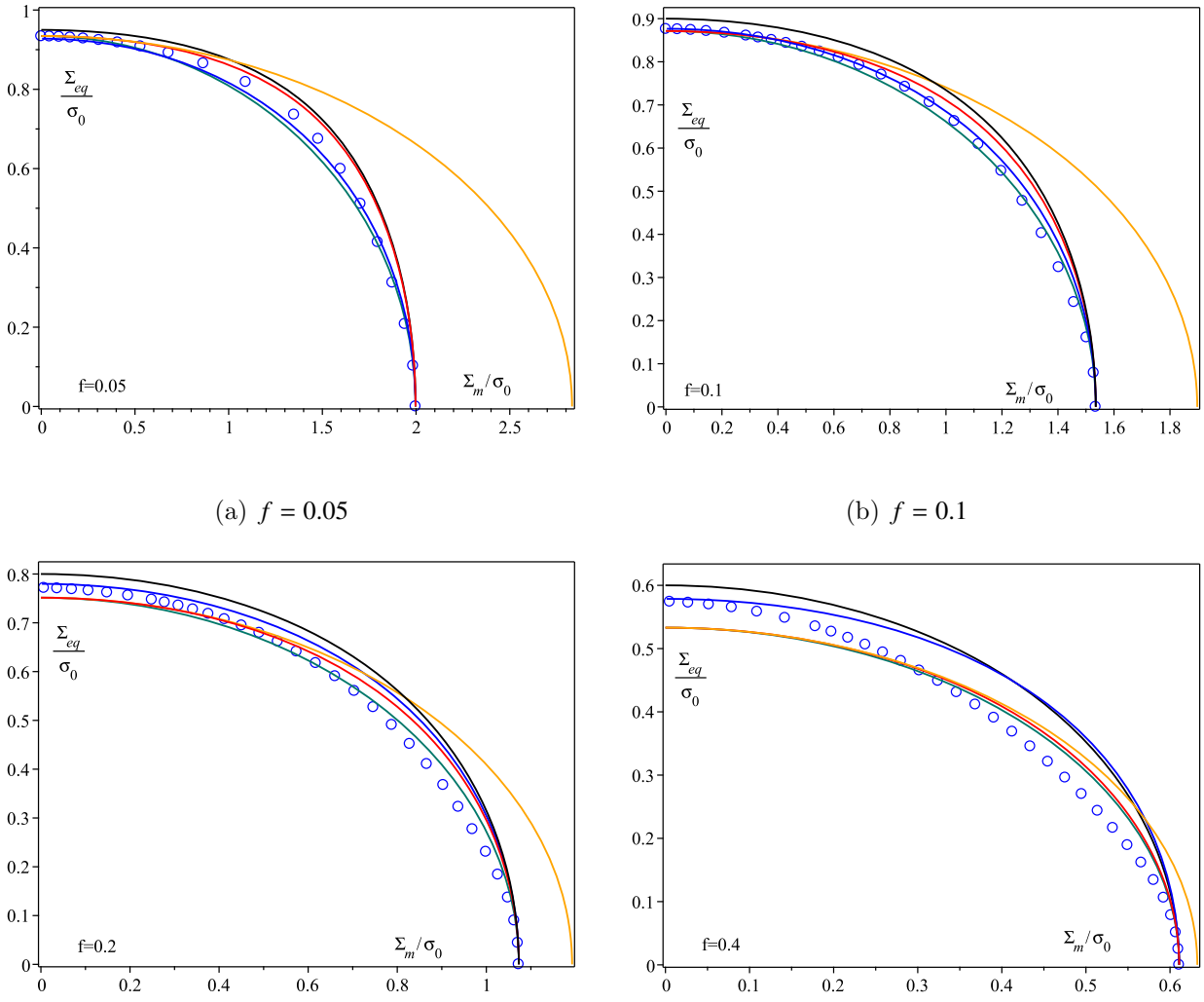

(a) $f = 0.05$ (b) $f = 0.1$

(c) $f = 0.2$ (d) $f = 0.4$

Figure 2: Comparisons between the FEM results (blue circle) and the predictions given by different criteria with different porosity $f = 0.05,\ 0.1,\ 0.2,\ 0.4$: black line - (2), red line - (3), orange line - (4), green line - (5), blue line - (6).

The main feature of the porosity effect on the macroscopic mechanical behavior is taken into account by these criteria, for example, the effective strength of porous materials decreases with the increase porosity f. But this influence has not been fully considered by these criteria for all range of porosity. To do this, a much richer velocity field is needed in the limit analysis method, or a more suitable stress field should be found for the stress

variational approach. These are hard works and it is not so easy to realize.

To overcome these difficulties, a machine leaning approach will be used in this work to study the influence of porosity f on the macroscopic mechanical behavior of porous materials.

4. Plastic yield surface of porous material predicted by Artificial Neuron Network

Inspired by the biological structure of neurons, the research of Artificial Neural Network (ANN) has been developed quickly since 1940s. According to the complexity of the studied problem, different architecture can be established in ANN with different neurons and different layers. Unlike the traditional method, there is few constraints in the modeling and it can find the mechanical behavior law behind the training data after the training procedure.

The problem presented in the above section 2 for the determination of the plastic yield surface can be regarded to find the relation between $\frac{\Sigma_m}{\sigma_0}$ and $\frac{\Sigma_{eq}}{\sigma_0}$ with the influence of porosity f. In view of ANN method, it can be treated as a regression problem. The studied propblem can be simplified as follows: according to the two input parameters: $\frac{\Sigma_m}{\sigma_0}$ and porosity f, one need to find the corresponding yield value of $\frac{\Sigma_{eq}}{\sigma_0}$ for the studied porous materials.

4.1. Principal technique of ANN method

In the architecture of artificial neuron network, there are mainly three parts: an input layer, hidden layers and an output layer. Different numbers of hidden layer and of neurons in each layer can be constructed according to the complexity of the studied problem. The general architecture of ANN for the present problem can be illustrated as in Figure 3. At the first input layer, there are two input parameters: $x_1 = f$, $x_2 = \frac{\Sigma_m}{\sigma_0}$. At the last output layer, there is one predictive yield value: $\frac{\Sigma_{eq}}{\sigma_0}$. For the hidden layers, different structure can be constructed.

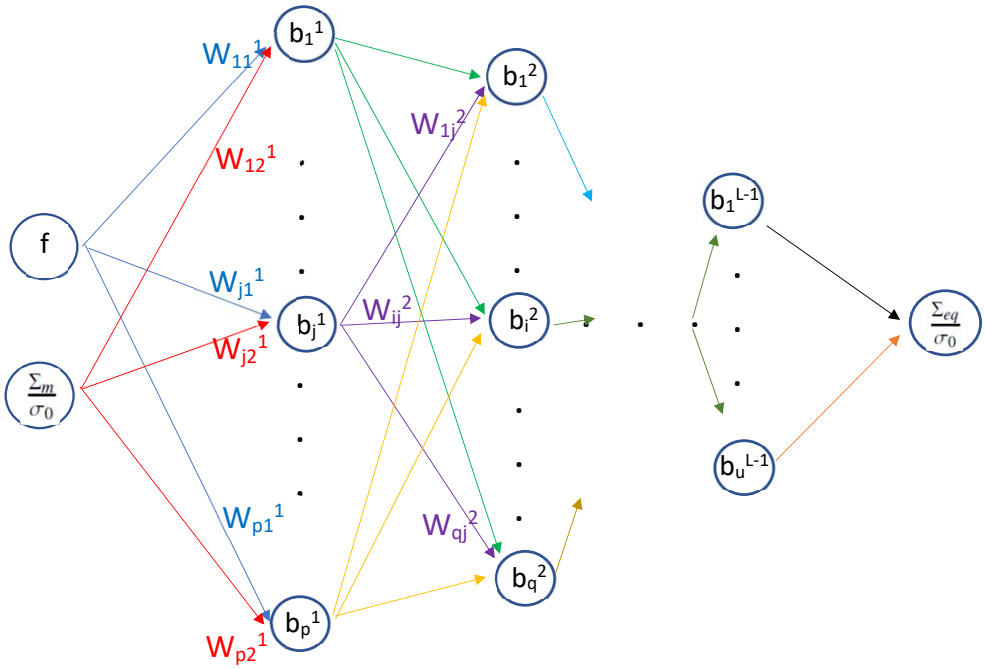

Figure 3: Architecture of artificial neuron network with L layer.

The neuron i in the layer l is connected to the one j located in the previous layer $l-1$ by the weight w_{ij}^l. There is no communication between the neurons in the same layer. It will receive the inputs x_j^{l-1} of all neurons in the previous layer. With the bias b_i^l of this neuron and the weights w_{ij}^l, the input of this neuron i at the layer l can be calculated as $z_i^l = \sum_{j=1}^{p} w_{ij}^l x_j^{l-1} + b_i^l$, where p is the total neuron number in the layer $l-1$. An activation function $a(z)$ is defined in each neuron to calculate the output of this neuron for the next layer $l+1$ by using the inputs z_i^l getting from previous layer $l-1$. For example, the output of a sigmoid neuron is given as:

$$a_i^l = \frac{1}{1+e^{-z_i^l}} = \frac{1}{1+e^{-\sum_{j=1}^{p} w_{ij}^l x_j^{l-1} - b_i^l}} \tag{7}$$

In view of the next layer $l+1$, a_i^l is an input which will be used to calculate its activation value with weights and biases. Following this procedure, we can get the final output value a at the last layer $l = L$ with the initial inputs x at the first layer $l = 0$. In order to measure the ANN output accuracy, a loss function is necessary. For the studied regression problem,

the mean squared error (MSE) loss function is adopted here:

$$C(w,b) = \frac{1}{2n}\sum_{i=1}^{n} \|a(x) - y\|^2 \tag{8}$$

in which n is the total number of training inputs; y is the true value with the input x and $a(x)$ is the one approximated by ANN method.

The initial values of weights and biases in the connection of neuron network are assigned randomly. Based on the training data, the purpose of the ANN method is to optimise the values of w and b by training process which minimize the cost function. By adopting the backpropagation algorithm [38], these values can be updated by the gradient descent:

$$\triangle w_{ij}^{l} = -\eta \frac{\partial C}{\partial w_{ij}^{l}}, \qquad \triangle b_{i}^{l} = -\eta \frac{\partial C}{\partial b_{i}^{l}}, \tag{9}$$

in which η is the learning rate. In order to speed up the learning procedure, the gradient of C over all the training inputs will be approximated by the one over a small number m (mini-batch) which are randomly chosen from training data. Many optimizations have been proposed for the gradient descent method and the learning rate [39–41], for example, Momentum-based gradient descent, Nesterov Accelerated Gradient (NAG), Adaptive subgradient method (AdaGrad), Adaptive Learning Rate Method (AdaDelta), Adaptive Moment Estimation (Adam) and so on. With the training procedure, the ANN method learns the law behind the training data and optimize the weights and biases in the architecture of the network.

The studied case can be treated as a regression problem of artificial neuron network. In order to evaluate the performance of the ANN performance, the coefficient of determination (R^2) between the true values and the predicted ones is chosen as the validation method:

$$R^2 = 1 - \frac{\sum_{i=1}^{m}(y_i - a_i)^2}{\sum_{i=1}^{m}(y_i - \bar{y})^2} \tag{10}$$

in which a_i denotes the ANN prediction, y_i is the true value, $\bar{y}$ the mean value of y_i and m the number of samples.

4.2. Training data

The training data used in artificial neuron network approach is a key point for the success. Due to its accuracy, the finite element method presented in the section 3 will be adopted to prepare the training and test data needed in ANN training procedure. A wide range of porosity f will be considered for the validation. The strategy of the data preparation are arranged as follows. There are two principal parts: the training data and the test data. The training data is used for the neuron network training process. For the purpose of validation, a sub set (10%) is chosen randomly from the training data used as the validation data to verify the accuracy of the training procedure. The porosities used in the training data are f = 0.005, 0.01, 0.02, 0.03, 0.04, 0.07, 0.1, 0.15, 0.2, 0.25, 0.3, 0.35, 0.4, 0.45, 0.5, 0.55, 0.6, 0.65, 0.7, 0.75, 0.8, 0.85, 0.9, 0.95. A wide range of stress triaxiality $T = \Sigma_m/\Sigma_{eq}$ are studied. After the training procedure, the weights and biases in the architecture of artificial neuron network are optimised based on the training data. Then, the prepared ANN can be used directly to predict the corresponding yield values of $\frac{\Sigma_{eq}}{\sigma_0}$ for a given porosity f and $\frac{\Sigma_m}{\sigma_0}$. Concerning the test data, FEM solutions with different stress triaxiality and different porosities from the ones used in training data are carried out, as f = 0.05, 0.19, 0.23, 0.33, 0.42, 0.51, 0.63, 0.72, 0.83, 0.92.

4.3. Predictions od plastic yield surfaces of porous medium by ANN approach

Based on these FEM results, the proposed artificial neuron network can be trained. Two hidden layers are chosen here. The architecture of ANN used is $(2 - 50 - 20 - 1)$ with the sigmoid activation function[1]. The number of mini-batch is taken as m = 100. With the optimization of Adam, the learning rate is taken as η = 0.005. The variations of the loss and the accuracy of the training set and validation set in training data are illustrated in Figure 4 as a function of the number of epoch[2]. One can see that the proposed neuron network converges very quickly. At the beginning, there are some fluctuations and the ANN learns

[1]The ANN model established in this study is based on the structure of open source code provided in https://github.com/microsoft/ai-edu

[2]A training epoch is one total computation of all training data.

from the training data. It adjusts itself and the loss drops quickly. At the same time, the accuracy increases rapidly. It is stable after about 10000 epoch. The final values of loss and accuracy are 0.6×10^{-5} and 0.99989 for the training set and 1.97×10^{-5}, 0.99964 for the validation set.

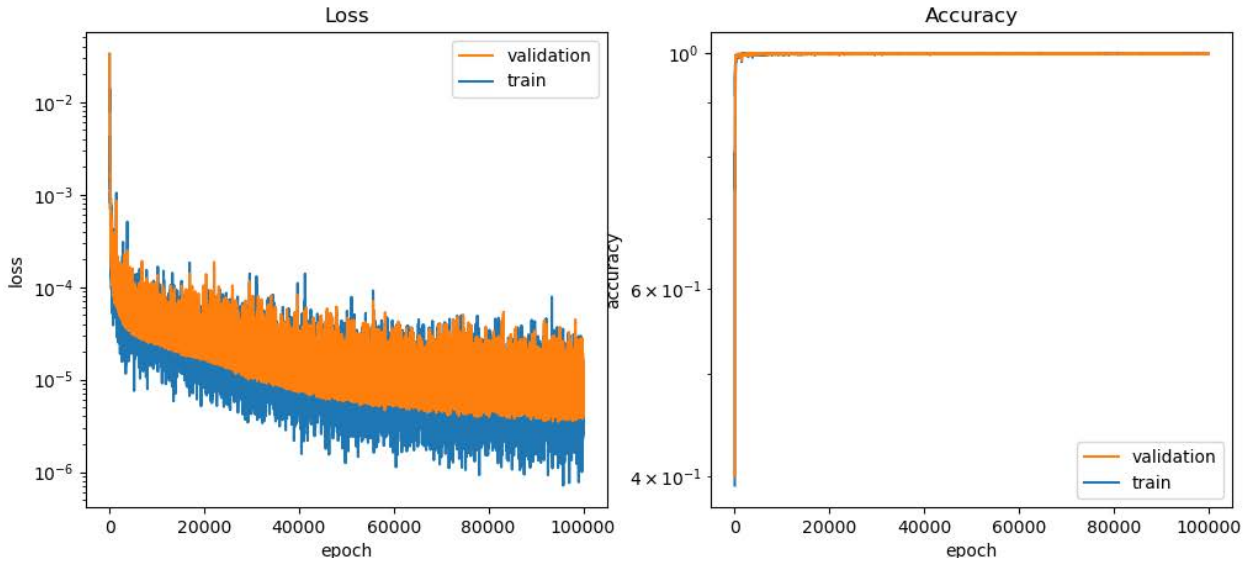

Figure 4: The variations of loss and accuracy of training set and validation set as a function of the number of epoch.

Figure 5 shows the comparisons between the FEM results (circle points) and the ANN predictions (solid lines) in the range of training data with different porosity f. A very good agreement is found between these two results for all porosities and all domains of stress triaxiality $T = \Sigma_m/\Sigma_{eq}$. The deviatoric and hydrostatic values are well captured. The mechanics of porous material, especially the influence of porosity on the macroscopic mechanical behavior and the relations between Σ_m and Σ_{eq}, are well accounted by the proposed artificial neuron network.

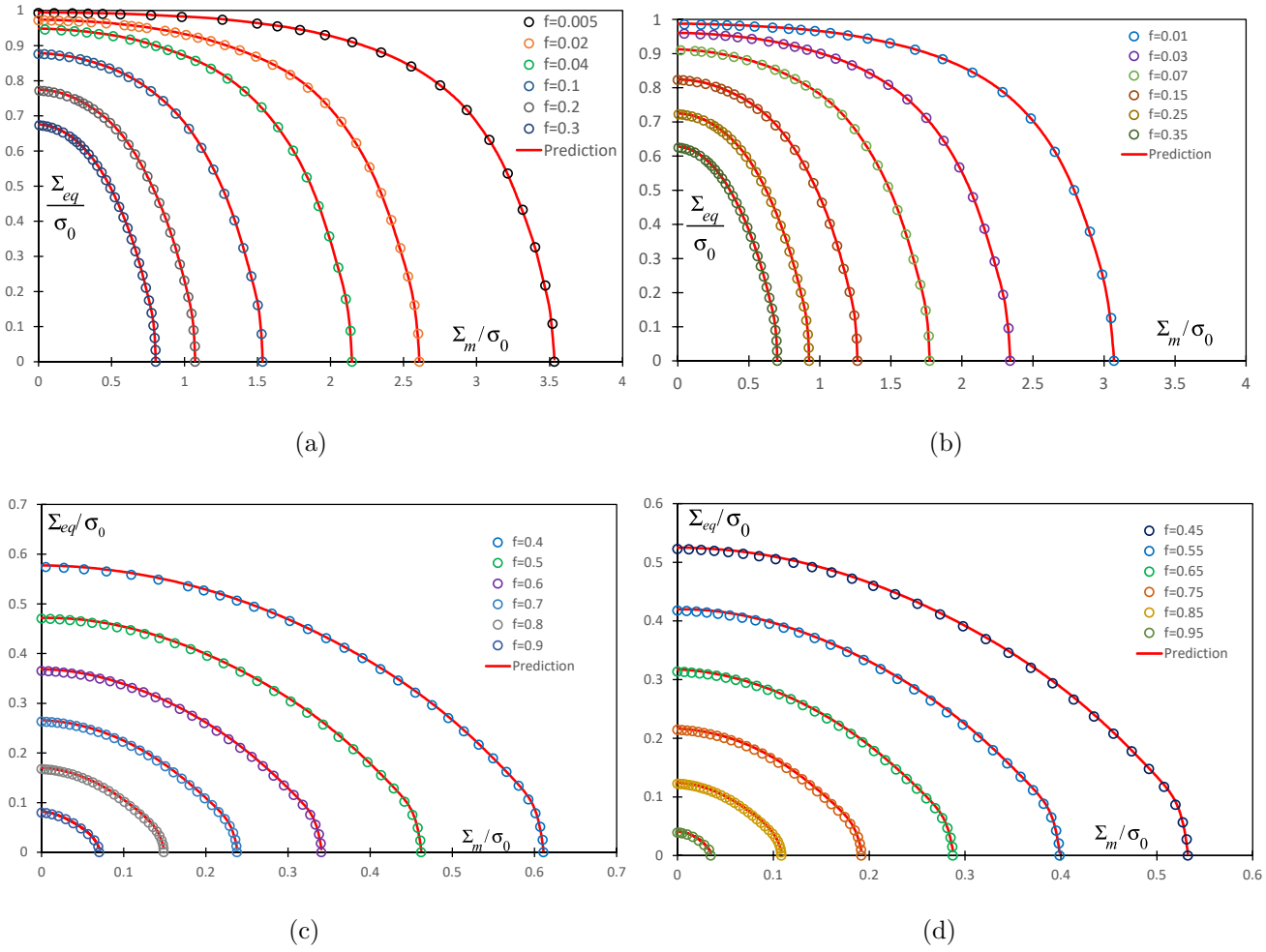

Figure 5: Comparisons between the FEM results (circle points) and the ANN predictions (solid lines) with different porosities f and stress triaxialities for training data.

The trained ANN now is applied to the test data in which the porosities f are totally different from the ones in the training data. The corresponding accuracy is **0.99975**. The comparisons between the FEM results (circle points) and the ANN predictions (solid lines)are illustrated in Figure 6 with different cases. The ANN prediction coincides well with the FEM results for both low and high porosities f. The mechanical features of porous material are well taken into account by the proposed ANN approach.

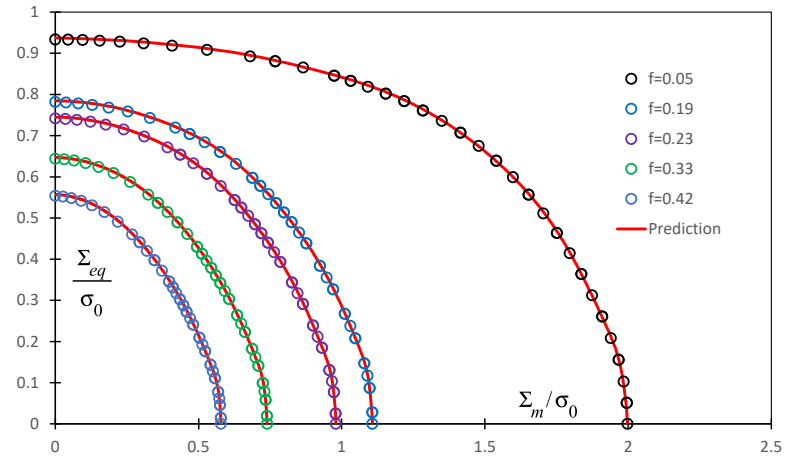

(a)

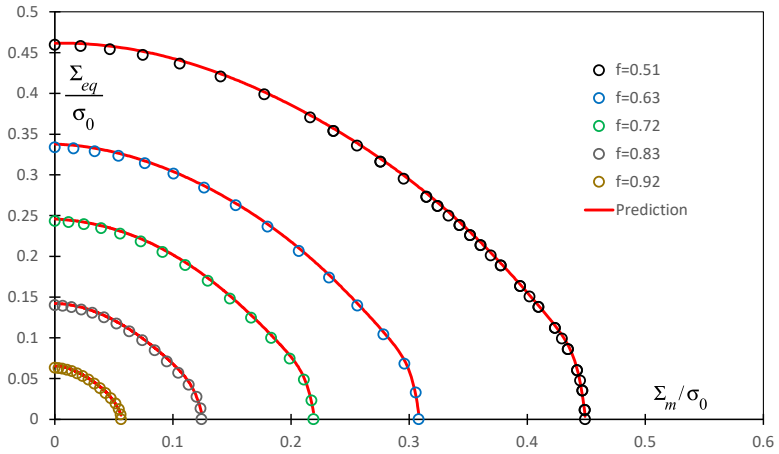

(b)

Figure 6: Comparisons between the FEM results (circle points) and the ANN predictions (solid lines) with different porosities f and stress triaxialities for test data.

It is now interesting to study the deviatoric value of $\frac{\Sigma_{eq}}{\sigma_0}$ for the case of $\frac{\Sigma_m}{\sigma_0} = 0$. As shown in the above section 2 for the analytical criteria, there are two main values predicted, as $\frac{\Sigma_{eq}}{\sigma_0} = 1 - f$ and $\frac{1-f}{\sqrt{1+2f/3}}$ obtained by different methods. As shown in Figure 7(a), circle points are FEM solutions, red solid line are ANN prediction, blue and green lines are two above values given by the analytical criteria respectively. The ANN prediction located between these two values and has a good agreement with numerical results for all range of porosity

f. The Figure 7(b) is for the comparisons for the hydrostatic value $\frac{\Sigma_m}{\sigma_0}$ when $\frac{\Sigma_{eq}}{\sigma_0} = 0$. For the studied porous material, one can calculated the exact analytical solution: $-\frac{2}{3}\ln(f)$. The ANN prediction (square points) has a good agreement with this exact solution (solid line).

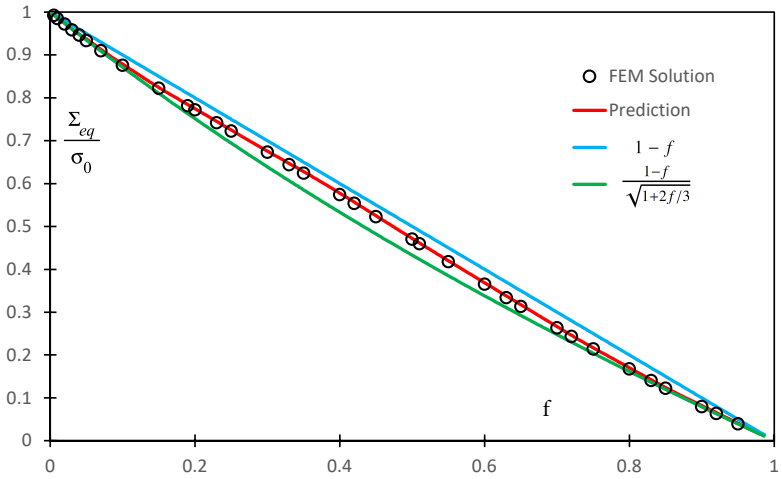

(a) Deviatoric value $\frac{\Sigma_{eq}}{\sigma_0}$ as function of f when $\frac{\Sigma_m}{\sigma_0} = 0$

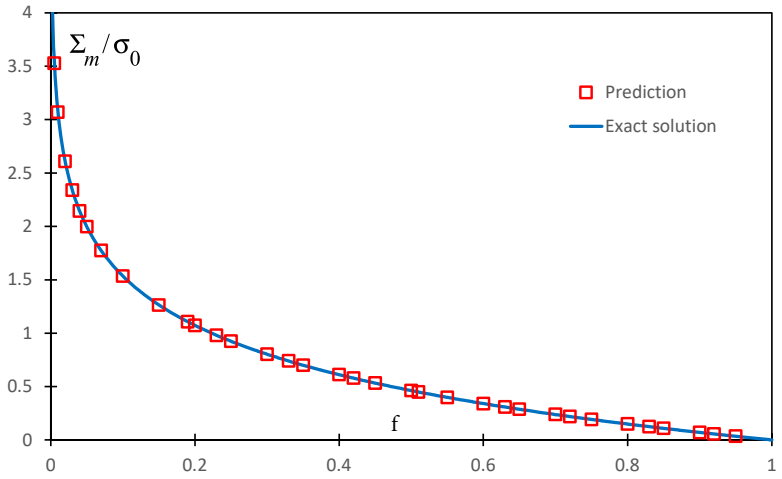

(b) Hydrostatic value $\frac{\Sigma_m}{\sigma_0}$ as function of f when $\frac{\Sigma_{eq}}{\sigma_0} = 0$

Figure 7: Comparisons of deviatoric value $\frac{\Sigma_{eq}}{\sigma_0}$ and hydrostatic value $\frac{\Sigma_m}{\sigma_0}$ between the FEM results and the ANN predictions as a function of porosity f.

5. Conclusions

The artificial neuron network is adopted in this paper to predict the macroscopic plastic yield surface of porous materials with a von Mises type solid matrix. The typical analytical yield criteria are firstly recalled. The main features of porosity effect on the macroscopic yield stress are taken into account by these criteria, such as the strength decrease with the increase of porosity, but it is not sufficient. However, it is a hard work to derive an explicit expression of yield criterion for the studied porous medium. For the purpose to get a better prediction, the ANN approach is adopted in this work. The studied problem can be seen as a regression problem with two inputs f and $\frac{\Sigma_m}{\sigma_0}$ and one output value $\frac{\Sigma_{eq}}{\sigma_0}$. The training procedure is a key step to optimise the weight and bias parameters. New numerical solutions for the studied porous material are presented with a wide range of porosity and macroscopic stress triaxiality, which are used as the training date and test one. The proposed ANN structure is well trained. There is a good agreement between the ANN predictions and FEM results. The prediction given by the ANN approach is much more accurate than the ones estimated by the existing yield criteria. The proposed ANN model is easy to use for practical applications.

Acknowledgement

This study was supported by the National Natural Science Foundation of China (Grant No.11902069), in part by the Young Talent Program of Liaoning Province under Grant XLYC1807094 and the framework of Sino-Franco Joint Research Laboratory on Multiphysics and Multiscale Rock Mechanics.

Appendix A. Parameters used in criterion (6)

$$P_0(f) = \frac{1 + \frac{11}{25}f - \frac{64}{75}f\ln(f) - \frac{2}{25}\sqrt{f}N + \frac{2}{375}fM}{1-f}$$

$$M = 105\cos\left(\tfrac{\sqrt{15}}{3}\ln(f)\right) + 17\sqrt{15}\sin\left(\tfrac{\sqrt{15}}{3}\ln(f)\right), N = 25\cos\left(\tfrac{\sqrt{15}}{6}\ln(f)\right) + \sqrt{15}\sin\left(\tfrac{\sqrt{15}}{6}\ln(f)\right) \tag{A.1}$$

$$P_1 = f - \frac{\sqrt{15f}}{25}\sin\left(\frac{\sqrt{15}}{6}\ln(f)\right) - \sqrt{f}\cos\left(\frac{\sqrt{15}}{6}\ln(f)\right) \tag{A.2}$$

$$\xi(\zeta) = \begin{cases} \frac{\sqrt{6}(2\sqrt{P_0}-\zeta)}{24\sqrt{\zeta P_0^{1/2}}}\ln\left(\frac{\sqrt{2\zeta(\zeta+P_0^{1/2})}+\sqrt{3}\zeta}{\sqrt{2\zeta(\zeta+P_0^{1/2})}-\sqrt{3}\zeta}\right) + \frac{1}{2}\frac{\sqrt{P_0^{1/2}+\zeta}}{P_0^{1/4}}, & \zeta \geq 0 \\ \frac{(2\sqrt{P_0}-\zeta)\arcsin\left(\frac{\sqrt{-3\zeta}}{\sqrt{2\sqrt{P_0}-\zeta}}\right)}{2P_0^{1/4}\sqrt{-6\zeta}} + \frac{1}{2}\frac{\sqrt{P_0^{1/2}+\zeta}}{P_0^{1/4}}, & \zeta \leq 0 \end{cases} \tag{A.3}$$

with $\zeta = sign(J_3)\frac{\frac{3\Sigma_m\Sigma_e\cdot\sqrt{P_0(f)}}{(1-f+P_1)\ln(f)}}{\frac{P_0(f)}{(1-f+P_1)^2}\Sigma_e^2 + \frac{9}{4\ln(f)^2}\Sigma_m^2}$

References

[1] A.L. Gurson. Continuum theory of ductile rupture by void nucleation and growth: part1-yield criteria and flow rules for porous ductile media. *J. Engrg. Mater. Technol.*, 99:2–15, 1977.

[2] V. Tvergaard. Influence of voids on shear bands instabilities under plane strain conditions. *Int. J. Fracture*, 17:389–407, 1981.

[3] V. Tvergaard. Material failure by void coalescence in localized shear bands. *Int. J. Solids Structures*, 18(8):659–672, 1982.

[4] P. Ponte Castaneda. The effective mechanical properties of nonlinear isotropic composites. *J. Mech. Phys. Solids*, 39:45–71, 1991.

[5] J-C. Michel and P. Suquet. The constitutive law of nonlinear viscous and porous materials. *Journal of the Mechanics and Physics of Solids*, 40:783–812, 1992.

[6] V. Monchiet, E. Charkaluk, and D. Kondo. A micromechanics-based modification of the Gurson criterion by using eshelby-like velocity fields. *European Journal of Mechanics - A/Solids*, 30(6):940–949, 2011.

[7] L. Cheng, G. de Saxcé, and D. Kondo. A stress-based variational model for ductile porous materials. *International Journal of Plasticity.*, 55:133–151, 2013.

[8] W.Q. Shen, A. Oueslati, and G. De Saxce. Macroscopic criterion for ductile porous materials based on a statically admissible microscopic stress field. *International Journal of Plasticity*, 70:60–76, 2015.

[9] M. Gologanu, J.B. Leblond, and J. Devaux. Approximate models for ductile metals containing non-spherical voids–cas of axisymmetric prolate ellipsoidal cavities. *J.Mech.Phys.Solids*, 41(11):1723–1754, 1993.

[10] M. Gologanu, J.B. Leblond, and J. Devaux. Approximate models for ductile metals containing non-spherical voids–cas of axisymmetric oblate ellipsoidal cavities. *ASME J.Eng. Mat. Tech.*, 116:290–297, 1994.

[11] S.M. Keralavarma and A.A. Benzerga. A constitutive model for plastically anisotropic solids with non-spherical voids. *Journal of the Mechanics and Physics of Solids*, 58:874–901, 2010.

[12] V. Monchiet, E. Charkaluk, and D. Kondo. Macroscopic yield criteria for ductile materials containing spheroidal voids: An eshelby-like velocity fields approach. *Mechanics of Materials*, 72:1–18, 2014.

[13] W.Q. Shen, J Lin, Q.Z. Zhu, V. Monchiet, and D Kondo. Macroscopic yield criterion for ductile materials containing randomly oriented spheroidal cavities. *International Journal of Damage Mechanics*, 20:1198–1216, 2011.

[14] W. Q. Shen, J. Zhang, J. F. Shao, and D Kondo. Approximate macroscopic yield criteria for drucker-prager type solids with spheroidal voids. *International Journal of Plasticity*, 99:221–247, 2017.

[15] H.Y. Jeong and J. Pan. A macroscopic constitutive law for porous solids with pressure-sensitive matrices and its implications to plastic flow localization. *Int. J. Solids Struct.*, 32:3669–3691, 1995.

[16] W.Q. Shen, F. Pastor, and D. Kondo. Improved criteria for ductile porous materials having a green type matrix by using eshelby-like velocity fields. *Theoretical and Applied Fracture Mechanics*, 67-68:14–21, 2013.

[17] T.F. Guo, J. Faleskog, and C.F. Shih. Continuum modeling of a porous solid with pressure sensitive dilatant matrix. *J. Mech. Phys. Solids*, 56:2188–2212, 2008.

[18] J.-F. Barthélémy and L. Dormieux. Détermination du critère de rupture macroscopique d'un milieu poreux par homogénéisation non linéaire. *C. R. Mecanique*, 331:271–276, 2003.

[19] S. Maghous, L. Dormieux, and J.F. Barthélémy. Micromechanical approach to the strength properties of frictional geomaterials. *European Journal of Mechanics A/Solid*, 28:179–188, 2009.

[20] W.Q. Shen, J.F. Shao, Z.B. Liu, A. Oueslati, and G. De Saxcé. Evaluation and improvement of macroscopic yield criteria of porous media having a drucker-prager matrix. *International Journal of Plasticity*, 126:102609, 2020.

[21] W. Q. Shen, J. F. Shao, D. Kondo, and G. De Saxce. A new macroscopic criterion of porous materials

with a mises-schleicher compressible matrix. *European Journal of Mechanics A/Solids*, 49:531–538, 2015.

[22] W.Q. Shen, J.F. Shao, A. Oueslati, G. De Saxcé, and J. Zhang. An approximate strength criterion of porous materials with a pressure sensitive and tension-compression asymmetry matrix. *International Journal of Engineering Science*, 132:1 – 15, 2018.

[23] P.-G. Vincent, Y. Monerie, and Suquet P. Ductile damage of porous materials with two populations of voids. *C.R.Mecanique*, 336:245–259, 2008.

[24] P.-G. Vincent, Y. Monerie, and Suquet P. Porous materials with two populations of voids under internal pressure: I. instantaneous constitutive relations. *Int J Solids Struct*, 46:480–506, 2009.

[25] W.Q. Shen, Z. He, L. Dormieux, and D. Kondo. Effective strength of saturated double porous media with a drucker-prager solid phase. *Int. J. Numer. Anal. Meth. Geomech.*, 38:281–296, 2014.

[26] W. Q. Shen and J. F. Shao. An elastic-plastic model for porous rocks with two populations of voids. *Computers and Geotechnics*, 76:194–200, 2016.

[27] W. Q. Shen, E. Lanoye, L. Dormieux, and D. Kondo. Homogenization of saturated double porous media with eshelby-like velocity field. *Acta Geophysica.*, 62(5):1146–1162, 2014.

[28] W. Q. Shen and J. F. Shao. An incremental micro-macro model for porous geomaterials with double porosity and inclusion. *International Journal of Plasticity*, 83:37–54, 2016.

[29] W.S. McCulloch and W. Pitts. A logical calculus of the ideas immanent in nervous activity. *Bulletin of Mathematical Biophysics*, 5:115–133, 1943.

[30] J. Ghaboussi, J. H. Garrett, and X. Wu. Knowledge-based modelling of material behaviour using neural networks. *ASCE Journal of Engineering Mechanics Division*, Jan., 1991.

[31] Tomonari Furukawa and Genki Yagawa. Implicit constitutive modelling for viscoplasticity using neural networks. *International Journal for Numerical Methods in Engineering*, 43(2):195–219, 1998.

[32] Zeliang Liu, C.T. Wu, and M. Koishi. A deep material network for multiscale topology learning and accelerated nonlinear modeling of heterogeneous materials. *Computer Methods in Applied Mechanics and Engineering*, 345:1138 – 1168, 2019.

[33] Sebastian Gajek, Matti Schneider, and Thomas Böhlke. On the micromechanics of deep material networks. *Journal of the Mechanics and Physics of Solids*, page 103984, 2020.

[34] S. Lee, J. Ha, M. Zokhirova, H. Moon, and J. Lee. Background information of deep learning for structural engineering. *Arch. Comput. Methods Eng.*, 25:121–129, 12018.

[35] L. Cheng and T. F. Guo. Void interaction and coalescence in polymeric materials. *Int. J. Solids Struct.*, 44:1787–1808, 2007.

[36] M. Trillat and J. Pastor. Limit analysis and Gurson's model. *Eur. J. of Mechanics*, 24:800–819, 2005.

[37] P. Thoré, F. Pastor, and J. Pastor. Hollow sphere models, conic programming and third stress invariant.

European Journal of Mechanics A/Solids, 30:63–71, 2011.

[38] D. Rumelhart, G. Hinton, and R. Williams. Learning representations by back-propagating errors. *Nature*, 323:533–536, 1986.

[39] J. Duchi, E. Hazan, and Y Singer. Adaptive subgradient methods for online learning and stochastic optimization. *Journal of Machine Learning Research*, 12:2121–2159, 2011.

[40] M. D. Zeiler. Adadelta: an adaptive learning rate method. *arXiv preprint*, arXiv:1212.5701, 2012.

[41] D. P. Kingma and J. Ba. Adam: A method for stochastic optimization. *arXiv preprint*, arXiv:1412.6980, 2012.